Organization of Spread Monolayers of Poly(lauryl methacrylate) at the Air–Water Interface from Neutron Reflectometry on Partially Labeled Isomers

I. Reynolds and R. W. Richards*

Interdisciplinary Research Centre in Polymer Science and Technology, University of Durham, Durham DH1 3LE, U.K.

J. R. P. Webster

Science Division, Rutherford Appleton Laboratory, Chilton, Didcot, Oxon OX11 0QX, U.K.

Received May 1, 1995; Revised Manuscript Received August 25, 1995®

ABSTRACT: Surface pressure isotherms of poly(lauryl methacrylate) (PLMA) spread monolayers at the air–water interface show that the thermodynamic state of the polymer is poorer than Θ conditions. Neutron reflectivity has been used to determine the organization of the polymer at the interface. To obtain maximum information, four variations of PLMA were synthesized, each with different isotopic labeling, and these were spread on two different aqueous subphases, D_2O and air contrast matched water. Reflectivities were recorded at two different surface pressures of 5 and 9 mN m^{-1}. Interpretation of these reflectivity profiles using the optical matrix calculation methods suggested a two-layer structure with the methacrylate backbone immersed in the subphase and the lauryl substituent protruding into the air phase but being penetrated to some extent by water. Direct analysis of the reflectivity data using partial structure factors allowed the dimensions, separations, and compositions of each of the layers to be determined. The backbone and substituent layers were describable by Gaussian distributions with standard deviations of 6 and 16 Å, respectively, at the highest surface pressure investigated. Over the same surface pressure range, the near surface water layer had a hyperbolic tangential organization. Separations between layers obtained from cross partial structure factors remained relatively unchanged as the surface pressure increased. The methacrylate backbone-rich and near surface water layers were separated by 2 Å, and the lauryl substituent-rich and water layer separation was ca. 6 Å. Methacrylate backbone and side chain distributions were separated by ca. 3 Å at 9 mN m^{-1}. These values were interpreted as indicative of complete immersion of the backbone and partial immersion of the lauryl substituents.

Introduction

Spread monolayers of polymers at the air–water interface are of interest for several reasons. They constitute quasi-two-dimensional systems and thus can be used to investigate the applicability of scaling theories where dimensionality is specifically incorporated into the expressions.[1] The interfacial properties of polymers in such situations determine the behavior of many systems, e.g., stabilization of emulsions, steric stabilization of colloidal dispersions,[2] and use of polymers for Langmuir–Blodgett films.[3] A detailed knowledge of the surface organization of polymers would contribute greatly to the manipulation and control of such systems to best advantage.

The majority of information available on spread polymer films has been obtained from surface pressure isotherms. These have been interpreted using equations of state,[4] and in some cases attempts have been made to deduce the detailed organization of the polymer from the surface pressure isotherms.[5] In all these cases it is assumed that the spread polymer film is homogenous; however, Barnes et al.[6–8] have provided evidence which shows that a surface pressure gradient can exist in the film. The magnitude and nature of this gradient are determined by several factors including the molecular weight of the polymer. Rondelez[9–11] was the first to apply scaling law ideas to the analysis of surface pressure isotherms, and these ideas were also used by Kawaguchi[12,13] in a series of publications concerning spread films of acrylic polymers.

Structural information about spread polymer films is much more scanty; in part this has been due to the restricted number of methods which can provide the information. Furthermore, the quantity of polymer in the spread film is so small that the signal obtained can be very weak. Brinkhuis and Schoutjens[14,15] have used ATR FTIR on spread films of stereoregular poly(methyl methacrylates) to deduce the orientation of the ester substituents. Ellipsometry has also been used on poly(methyl methacrylate)[16] spread films and on poly(isopropylacrylamide) films to determine thickness.[17] A problem with these latter results is that severe assumptions often need to be made to interpret the data. Indeed, Stamm et al.[18] maintain that these assumptions are so severe that simultaneous evaluation of the thickness and refractive index of the spread polymer layer is not possible.

Reflectivity techniques respond to the thickness and composition of thin films and major advances in the understanding of surfactant excess layers at the air–water interface have been made in the last few years.[19–21] Although X-ray reflectivity has played a role in this, the most significant contributions have been due to the application of neutron reflectivity and taking full advantage of the benefits due to selective labeling. In earlier papers we reported[22,23] the application of neutron reflectometry to spread films of the tactic isomers of poly(methyl methacrylate) and poly(ethylene oxide). In some of that work limited use was made of the kinematic approximation and the partial structure factor description of the reflectivity.[24] Subsequently, we made

* To whom correspondence should be addressed.

® Abstract published in *Advance ACS Abstracts,* October 15, 1995.

0024-9297/95/2228-7845$09.00/0

a fuller use of partial structure factors when discussing spread films of a linear diblock copolymer of poly(methyl methacrylate) and poly(ethylene oxide) at the air–water interface.[25] We discuss here the organization of poly(lauryl methacrylate) (PLMA) at the air–water interface at 298 K. Neutron reflectometry has been used in conjunction with PLMA polymers deuterium labeled in the backbone, the substituent, or both parts of the molecule. The combination of a hydrophobic long alkyl group with a hydrophilic carbonyl residue leads to surface structure considerably different from that of poly(methyl methacrylate). An outline of the theory of neutron reflectivity is provided with special emphasis on the use of partial structure factors. We emphasize here that the full power of this method has been demonstrated by the work of Thomas and colleagues[19,21,26,27] on surfactant layers, and these papers should be consulted for full details.

Theory of Neutron Reflectivity

When neutrons are incident at glancing angles on a liquid surface, the reflected beam is composed of specularly reflected and scattered neutrons from the near surface region and the bulk subphase, respectively. The scattered neutrons create a background, which when subtracted from the total reflected intensity leaves the reflectivity of the system. The variation of the reflectivity with incident angle is discussed in terms of the scattering vector (or momentum transfer, $h(Q)$ ($Q = (4\pi/\lambda) \sin\theta$, where λ is the neutron beam wavelength and θ the glancing angle of incidence), normal to the surface. The reflectivity, $R(Q)$, is determined by the neutron refractive index normal to the surface, and this is controlled by the scattering length density distribution normal to the surface. It is the local concentration of species at the depth z which determines the variation of scattering length density and hence $R(Q)$ with Q which thus contains information about the composition profile normal to the surface of the liquid subphase. Optical matrix methods[28] can be used to calculate the neutron reflectivity exactly for any scattering length density profile normal to the interface provided that the profile can be described by a series of lamina of defined thickness and scattering length density.

However, more than one model may give the same reflectivity profile since thickness and scattering length density are coupled in the optical matrix expressions. To some extent this can be overcome by optimizing the same model to reflectivity profiles obtained using several different contrast conditions by using isotropic substitution of both the polymer and the subphase. A more direct method of analyzing reflectivity profiles obtained under different contrast conditions is to use the kinematic approximation and partial structure factors.[19–21,26,27] It is then possible to obtain the thickness, number density, and relative location of the different constituents which make up the near surface layer. These layers may be discrete components (e.g., cosolvent or ionic species) or different parts of the same molecular species.

For a macroscopically smooth surface the specular reflectivity in the kinematic approximation is given by

$$R(Q) = \left(\frac{16\pi^2}{Q^2}\right)|\rho(Q)|^2 \tag{1}$$

Where $\rho(Q)$ is the one-dimensional Fourier transform of $\rho(z)$, the scattering length density normal to the surface at the depth z.

$$\rho(Q) = \int_{-\infty}^{\infty} \exp(-iQz)\rho(z)\, dz \tag{2}$$

An alternative to eq 1 can be written in terms of the gradient of the composition distribution, $d\rho(z)/dz = \rho'(z)$

$$R(Q) = \left(\frac{16\pi^2}{Q^4}\right)|\rho'(Q)|^2 \tag{3}$$

This form is advantageous for the analysis of reflectivity data since $Q^4R(Q)$ generally has a strong maximum at a value of Q determined by the layer dimensions being considered. The scattering length density at any point in the distribution is given by

$$\rho(z) = \sum n_i(z)b_i \tag{4}$$

With n_i the number density of species i with a scattering length b_i. For the system considered here, i.e., poly(lauryl methacrylate) spread at the air–water interface, we consider the distribution of three components, the methacrylate backbone (b), the lauryl side chains (c), and the aqueous subphase (w). The scattering length density in the near surface layer can be written in terms of these three components as

$$\rho(z) = n_b(z)b_b + n_c(z)b_c + n_w(z)b_w \tag{5}$$

Taking the one-dimensional Fourier transform of eq 5 to obtain $\rho(Q)$ and substituting into eq 1, then

$$R(Q) = \frac{16\pi^2}{Q^2}[b_b{}^2h_{bb}(Q) + b_c{}^2h_{cc}(Q) + b_w{}^2h_{ww}(Q) + 2b_bb_ch_{bc}(Q) + 2b_bb_wh_{bw}(Q) + 2b_cb_wh_{cw}(Q)] \tag{6}$$

where $h_{ii}(Q)$ and $h_{ij}(Q)$ are, respectively, the self and cross partial structure factors which are the one-dimensional Fourier transforms of the number density distributions normal to the surface

$$h_{ii}(Q) = |n_1(Q)^2| \tag{7}$$

$$h_{ij}(Q) = \mathrm{Re}|n_i(Q)n_j{}^*(Q)| \tag{8}$$

It was remarked earlier that the reflectivity can be expressed in terms of $\rho'(Q)$; similarly eq 6 can be written in a derivative form where

$$h_{ii}{}'(Q) = Q^2h_{ii}(Q) \tag{9}$$

and

$$R(Q) = \frac{16\pi^2}{Q^4}[b_b{}^2h_{bb}{}'(Q) + b_c{}^2h_{cc}{}'(Q) + b_w{}^2h_{ww}{}'(Q) + 2b_bb_ch_{bc}{}'(Q) + 2b_bb_wh_{bw}{}'(Q) + 2b_cb_wh_{cw}{}'(Q)] \tag{10}$$

The self partial structure factors contain information about the distribution of each of the components in the near surface layer but no information regarding their relative positions with respect to each other. It is the cross partial structure factors which contain information about the relative positions of the various components.

In eqs 6 and 10 there are six partial structure factors and therefore to obtain each of these, six reflectivity profiles must be obtained under different contrast conditions, i.e., where the scattering length density of each component of the polymer and that of the subphase is varied. A series of simultaneous equations can then

be solved to give $h_{ii}(Q)$ and $h_{ij}(Q)$ as a function of Q. Such variations of contrast are realized by replacing hydrogen by deuterium in the polymer molecules and using two different subphases, D_2O and null reflecting water (NRW), the latter being a combination of H_2O and D_2O to produce water of zero scattering length density. When the subphase has a nonzero scattering length density, Crowley[29] has shown that the reflectivity to be used in the solution of either eq 6 or 10 must be scaled by values of the reflectivity calculated for the perfectly smooth subphase using the kinematic reflectivity ($R_k(Q)$ calculated from eq 1) and the exact Fresnel ($R_f(Q)$) reflectivity, the latter being calculated by optical matrix methods. Thus the reflectivity required when the polymer is spread on D_2O is given by

$$R(Q) = R_k(Q) + \left[\frac{R_{exp}(Q) - R_f(Q)}{1 - R_f(Q)}\right]\left[\frac{1 + (1 - Q_c^2/Q^2)^{1/2}}{2}\right]^2 \quad (11)$$

with Q_c the critical value of the scattering vector below which total reflection is observed and $R_{exp}(Q)$ the experimentally observed reflectivity.

Experimental Section

Synthesis of Polymers. Four isotopic variants of PLMA were synthesized. These consisted of polymers which were fully hydrogenous (HMHL), fully deuterated (DMDL), or combinations of the two, i.e., deuterated methacrylate backbone with hydrogenous lauryl ester groups (DMHL) and hydrogenous methacrylate backbone with deuterated lauryl ester groups (HMDL).

For synthesis of the fully hydrogenous polymer, lauryl methacrylate (0.2 mol) was dissolved in 500 mL of 2-butanone. The solution was brought to boiling point under a nitrogen atmosphere, and AIBN (0.001 mol) was added. The solution was refluxed for 6 h before being reduced in volume, allowed to cool, and then poured into a large excess of methanol. Conversion of monomer to polymer was 58%. Size exclusion chromatography (SEC) gave a weight-average relative molar mass of 37 600 and a polydispersity of 1.97.

To obtain a narrow molecular weight distribution polymer, the PLMA was fractionated by dissolving in 2-butanone to form a 1% w/v solution which was placed in a thermostat bath set at 298 K. Aliquots of methanol were added to the stirred solution until it became turbid, and the temperature was then raised by 15 K to redissolve the precipitate. Stirring was then ceased and the solution was allowed to cool to 298 K overnight. The precipitated polymer settled to the bottom, from where it was removed. Seven fractions were obtained in this way; a last fraction was recovered by removal of the solvent. Each fraction was analyzed by SEC, and one was selected for use in the surface pressure and neutron reflectometry experiments detailed below.

Synthesis of the deuterated polymers required prior synthesis of the respective monomer. Each monomer was prepared by transesterifying methyl methacrylate with lauryl alcohol, using either hydrogenous or deuterated methacrylate or alcohol depending on which part of the resulting polymer was to be labeled. In each case the same procedure was used for the transesterifications. Lauryl alcohol (ca. 0.02 mol) was dissolved in 90 mL of anhydrous THF, and the solution was placed in an ice bath and flushed continuously with dry nitrogen. An equimolar amount of *n*-butyllithium (2 M solution) was added to the lauryl alcohol, followed by methyl methacrylate (ca. 0.025 mol). The reaction was then left for 2 h, after which the solution was filtered to remove solids and the THF removed by rotary evaporation. Each reaction yielded about 0.014 mol of labeled LMA, and analysis by IR and NMR methods confirmed that the products were pure and deuterium labeled in the desired positions. The same procedure as used for the synthesis of the fully hydrogenous polymer was used to prepare the partially labeled polymers. The polymers were not fractionated due to the small amounts obtained, and the results of SEC analysis on all polymers used here are given in Table 1. From ^{13}C NMR analysis of each polymer the tacticities were similar in all cases, being 65% syndiotactic, 33% atactic, and 2% isotactic.

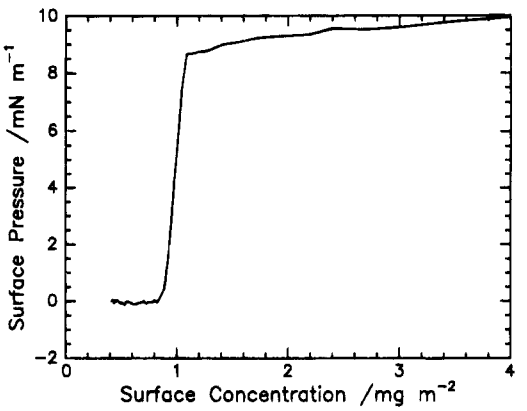

Figure 1. Surface pressure isotherm for PLMA at 298 K.

Table 1. Relative Molar Masses and Polydispersities of Poly(lauryl methacrylates)

polymer	$\bar{M}_w$	$\bar{M}_n$	$\bar{M}_w/\bar{M}_n$
DMHL	165 100	111 600	1.48
HMDL	62 900	44 300	1.42
DMDL	81 700	55 200	1.48
HMHL	176 000	159 100	1.10

Surface Pressure Isotherms. Surface pressure isotherms were obtained using a NIMA Langmuir trough (NIMA Technology, Coventry, UK) which consisted of a circular Teflon trough with motorized barriers and a pressure sensor to which a Wilhelmy plate was attached to measure the surface pressure of the spread polymer on the water surface. The temperature of the trough was maintained at 298 K by circulating water from a thermostated water bath through a labyrinth of channels in contact with the bottom of the trough.

The polymer was spread on the water subphase from chloroform solutions with a polymer concentration of ca. 1.00 mg mL^{-1}. Typically, 20 μL of this solution was dispensed onto the subphase, corresponding to an initial surface concentration of ca. 0.23 mg m^{-2} over the trough area of 900 cm^2. The monolayer was compressed at a speed of 30 cm^2 min^{-1}, but we found no influence of compression rate up to barrier speeds of 100 cm^2 min^{-1}, which was the maximum investigated. Additionally, neither differences in molar mass nor deuterium content of the various polymers produced any variation in the surface pressure isotherms.

Neutron Reflectivity. Neutron reflectivity experiments were carried out on the CRISP reflectometer at the UK pulsed neutron source, ISIS, at the Rutherford Appleton Laboratory, which has been described in detail elsewhere.[30] For the experiments described here a neutron beam with a wavelength distribution from 0.5 to 6.5 Å was used with an incident angle of 1.5° on the aqueous subphase. The momentum transfer (Q) range explored was 0.05–0.65 Å^{-1}. The beam dimensions used were 40 mm wide × 2.5 mm high, and the intensity of specularly reflected neutrons was detected by a single time-of-flight detector. A rectangular NIMA Langmuir trough covered by a Perspex lid with quartz inlet and outlet windows was placed in the neutron beam path. Each isotopic variant of the polymer was spread on D_2O, whereas only the deuterated (or partially deuterated) variants were spread on null reflecting water (NRW).

Results

Surface Pressure Isotherms. A typical surface pressure isotherm is shown in Figure 1. Extrapolation of the surface pressure to zero gives a limiting surface concentration (Γ_{lim}) of 1.04 ± 0.02 mg m^{-2}, from which we calculate the limiting area per polymer segment to be 40.5 ± 0.5 Å^2/segment.

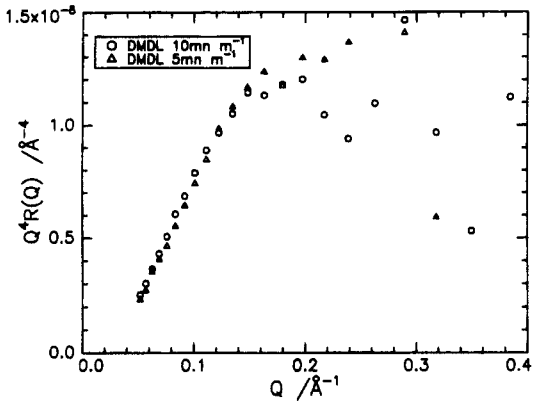

Figure 2. Reflectivity data plotted as RQ^4 for the DMDL polymer on NRW: (O) 9 mN m^{-1}; (△) 5 mN m^{-1}.

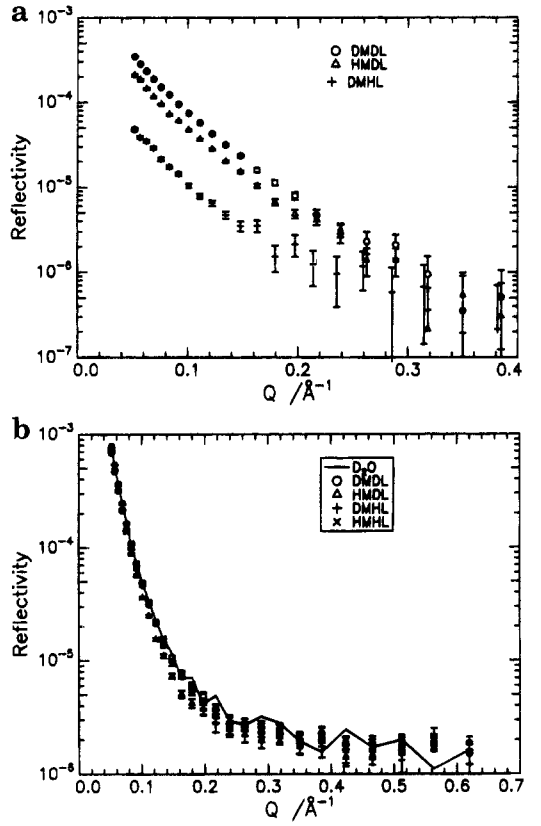

Figure 3. Neutron reflectivity profiles for each polymer on NRW and D_2O at a surface pressure of 9 mN m^{-1}. (a) On NRW [(O) DMDL; (△) HMDL; (+) DMHL] and on D_2O [(×) HMHL; (+) DMHL; (O) DMDL; (△) HMDL. The solid line is the reflectivity for D_2O alone.

Neutron Reflectivity. For each polymer, reflectivity profiles were obtained at two surface pressures of 5 and 9 mN m^{-1}, corresponding to the transition ($1 \leq \Gamma \leq 1.2$ mg m^{-2}) and high concentration ($\Gamma > 1.2$ mg m^{-2}) regions of the $\pi-\Gamma$ isotherms, respectively. Reflection profiles for the fully deuterated polymer on NRW at 5 and 9 mN m^{-1} are shown in Figure 2. The data are plotted in $Q^4R(Q)$ form to magnify any potential differences in the reflectivities; even by this method the differences are very subtle and barely noticeable at low Q values. The influence of the deuterium labeling on the reflectivity is shown in Figure 3a for a surface pressure of 9 mN m^{-1}, and the effect of the scattering length densities of the constituent parts of the lauryl methacrylate segment (Table 3) is clearly evident in these reflectivity profiles. Reflectivity profiles for each isotopic variant spread on D_2O at a surface pressure of 9 mN m^{-1} are shown in Figure 3b. These profiles are typical for both surface pressures investigated in that for each polymer at both surface pressures, the reflectivity is similar to clean D_2O, with little or no variation being observed in the reflectivity, especially for Q values below 0.1 Å^{-1}.

Discussion

Prior to discussion of these data and description of the organization which results from the analysis, it is pertinent to outline some of the aspects which motivated this investigation. There were two main reasons for our choice of this polymer: first, to investigate the application of the kinematic approximation to polymers (rather than small molecules) to determine whether information of the same level of detail as that obtained for surfactants was accessible and second, to determine whether the large lauryl substituent caused a different surface organization of the backbone relative to the air–water interface compared to that of poly(methyl methacrylate). Additionally, we also wished to determine whether there was any straightening of the lauryl side chains as the surface concentration of the polymer increased. The nature of the surface pressure isotherm for PLMA is rather similar to that observed for poly(dimethylsiloxane) spread on water[31] in that a surface pressure of zero is recorded at small but finite surface concentrations. An abrupt increase in surface pressure takes place over a very small range of surface concentration and then a plateau forms corresponding to the fully compressed polymer film. Applying the scaling law relation

$$\pi \propto \Gamma^{y} \tag{12}$$

to the surface pressure data between surface concentrations of ~1–1.1 mg m^{-2} i.e., above c^*. In equation 12, $y = 2\nu/(2\nu - 1)$ and the value of the scaling exponent ν relates to the thermodynamic state of the polymer. When the polymer–subphase interaction is thermodynamically favorable (excluded volume limit), then $\nu = 0.75$. Although a range of values have been proposed for the value of ν under two-dimensional Θ state conditions, an accepted value appears to be 0.57.[22] From the surface pressure data obtained here, we obtain a value of 0.53 for ν, which suggests that the PLMA molecules are in a collapsed state. However, we have pointed out in an earlier publication[32] the uncertainties in obtaining the exponent ν from π,Γ data. The value of ν obtained for the current data is very similar to that obtained for syndiotactic poly(methyl methacrylate).

The abrupt increase in surface pressure lends credence to the idea that at low concentrations the spread polymer exists as "islands" or droplets on the surface, a situation which has also been attributed to spread films of poly(methyl methacrylate).[16] Only when the islands contact each other and a coherent film is formed does the surface pressure increase. In this respect it is worth noting that the glass transition temperature of PLMA is ca. 180 K and hence the molecules have sufficient mobility for the "islands" to relax and interpenetrate rapidly on contact. We note here that evidence for the existence of islands of PLMA at low surface concentration appears to be confirmed by our separate experiments on the time variation of the intensity of light scattered from the surface of water on which PLMA has been spread.[33]

Because of the possible existence of islands of spread polymer at very low surface concentrations (<1 mg m^{-2}), we confine our discussion of the neutron reflectometry data to those reflectivity profiles obtained at a surface pressure of 5 and 9 mN m^{-1}. Before proceeding to a

Table 2. Scattering Lengths and Scattering Length Densities of Subphase Constituents, Backbone Segment, and Substituent Segment

component	scattering length/10^{-4} Å	scattering length density/10^{-6} Å^{-2}
D_2O	1.92	6.35
H_2O	−1.68	−0.56
DMDL	31.8	6.6
HMHL	0.58	0.31
DMHL	5.79	1.46
HMDL	26.61	5.66
HM	1.62	1.20
DM	6.82	5.35
HL	−2.38	−0.26
DL	23.65	7.24

quantitative analysis of the reflectivity data, we set out possible options for the arrangement of PLMA at the air−water interface and attempt to draw some conclusions from the reflectivity profiles for each of these options. To aid this process we refer to the scattering length densities of each of the polymers, the separate constituent parts (backbone, substituent) and subphase constituent given in Table 2.

Possible arrangements of PLMA at the air−water interface are (1) a layer where both substituent and backbone are mixed homogeneously but with no additional components in the layer, e.g., subphase; (2) as in (1) but also containing a proportion of subphase; (3) an arrangement where the lauryl substituent occupies a different spatial region from the methacrylate backbone; (4) as in (3) but with subphase distributed in each of the layers.

For simplicity, in the first instance we consider the separation between backbone and substituent regions in options 3 and 4 to be sharp. Since the polymer is well above its T_g and we are considering only monolayers where the surface concentrations are relatively high, then the possibility of air being in the polymer layer is excluded. Comparing the reflectivity profiles for the deuterium-labeled polymers on NRW (Figure 3a), the reflectivity values are ordered according to the scattering length density values in Table 2. The ratios of the reflectivities at $Q = 0.1$ Å^{-1} are not in exact agreement with the ratios of the scattering length densities, the experimental reflectivity ratios being slightly lower than the commensurate ratios of the scattering length densities. This indicates that the PLMA layer contains material in addition to the PLMA and hence arrangement 1 can be rejected. We next consider the same polymers and the fully hydrogenous polymer spread on D_2O. Since DMDL has a scattering length density approximately that of D_2O and that of HMHL is approximately zero, then we anticipate that these two polymers, when spread on D_2O, would produce a reflectivity little different from that of clean D_2O. This is borne out by a comparison of the reflectivity profiles with that of D_2O (Figure 3b). Referring to Table 2, it would appear that the DMHL polymer spread on D_2O should result in a reflectivity which is smaller than that of D_2O. The HMDL polymer should have a reflectivity very slightly reduced from that of D_2O. These anticipations are made on the basis of a uniform composition single layer. In fact, what is observed is quite contrary to the expectations based on scattering length density values. It is the HMDL spread polymer which produces a lower reflectivity and the DMHL spread polymer has a reflectivity little changed from that of D_2O. These observations can be qualitatively accounted for by invoking a two-layer model, i.e., (3) or (4) above. From Table 2 the hydrogenous substituent (HL) has a scattering length density which we can approximate to zero. The deuterated backbone (DM) has a scattering length density which approaches that of D_2O. Hence when the DMHL polymer is spread on D_2O, as long as the upper layer (i.e., that nearer the air) is the lauryl substituent layer, we anticipate little change in the reflectivity compared to D_2O. On the assumption that this same arrangement of backbone and substituent persists in the HMDL spread polymer, a different reflectivity profile would be expected due to the different distribution of scattering length density normal to the air−water interface. The distributions in scattering length density resulting from this anticipated arrangement are shown in Figure 4, and we compare *calculated* reflectivities from these two models with that calculated for clean D_2O in Figure 5. Note in these calculated reflectivity profiles we have not included any contribution due to background intensity arising from incoherent scattering of neutrons by the spread polymer/subphase combination. In making these calculations, we have used 16 Å

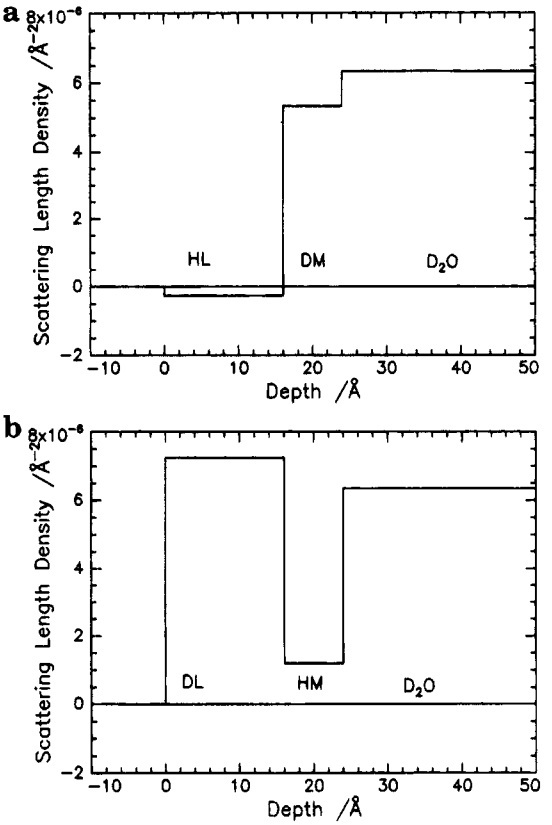

Figure 4. Schematic scattering length density distributions for (a) DMHL and (b) HMDL polymers spread on D_2O.

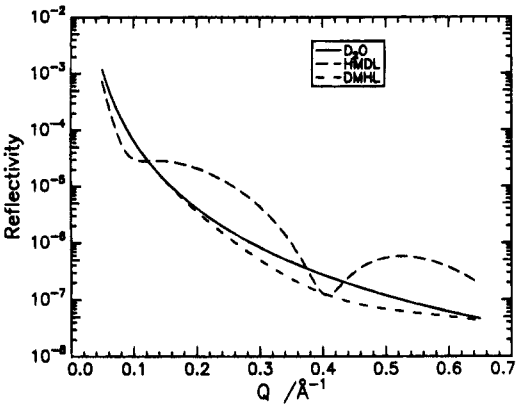

Figure 5. Reflectivities calculated by the exact optical matrix method from the scattering length density distributions of Figure 4.

Table 3. Layer Thickness and Scattering Length Density from Fit of Two-Layer Model for Reflectivity Profiles on NRW at $\pi = 9$ mN m^{-1}

polymer	t_u/Å	$\rho_u/10^{-6}$ Å^{-2}	t_l/Å	$\rho_l/10^{-6}$ Å^{-2}
DMDL	11	5.0	11	1.7
HMDL	11	4.7	11	1.1
DMHL	11	−0.1	9	1.8

as the thickness of the substituent layer and 8 Å as the thickness of the backbone layer, these being reasonable values based on computer models of the polymer. From Figure 5 it is clear that at low Q we cannot distinguish between the reflectivities of clean D_2O and DMHL spread on D_2O. Additionally, the HMDL reflectivity is initially lower than that of D_2O. At higher Q, comparison with experimental data is difficult because of the contribution from background signal. However, if the arrangement at the surface was as sharp as that implied by Figure 4, we should be able to see traces of the first maximum in the reflectivity. The absence of this feature is attributable to two factors either in combination or separately. First, we know from the discussion of the reflectivity profiles of the polymers spread on NRW that the polymer layer contains subphase. Consequently, the "hole" in the scattering length density profile of Figure 4 due to the hydrogenous backbone will not be so deep. Second, and more importantly, the interfaces between substituent layer and backbone layer and between subphase and backbone layer will not be sharp, and this will smooth the reflectivity profile considerably and any minima will be lost.

Summarizing our conclusions from inspections of the reflectivity profiles in conjunction with a knowledge of the scattering length densities and some coarse-grained simulations, it appears that PLMA arranges itself at the air−water interface with the lauryl substituents closer to the air. The methacrylate backbone is closest to the water and may be immersed in the subphase. Substituent and backbone do not occupy totally separate regions of space normal to the interface and there appears to be a finite extent of intermixing between them.

A two-layer model can be fitted to the reflectivity profiles for the deuterium-labeled polymers spread on NRW using the exact optical matrix method. The fitting was optimized for all three deuterated polymers spread on NRW, and the optimized parameters of the fits (layer thickness and scattering length density) are given in Table 3. Figure 6 shows the agreement between the experimental and calculated reflectivity. These reflectivity data have had incoherent background subtracted from them and consequently reflectivity data for Q values greater than 0.4 Å^{-1} are subject to random fluctuations since the values are very close to background here. This is especially true for the DMHL polymer on NRW where the reflectivity was very low. The background signal subtracted from the reflectivities was the average reflectivity calculated for the six highest Q values used. From the values in Table 3 we can make the following conclusions. The upper layer primarily contains the lauryl substituent since fitting to the DMHL reflectivity produces a negative scattering length density. However, the value is more positive than the value for a pure HL layer. This increase in scattering length density may be due to the presence of subphase and/or backbone in the substituent layer. Since we know that a sharp interface between the two layers does not exist, this argues for partial mixing with the backbone layer. Considering the fitted scattering length densities for DMDL spread on NRW, it is evident

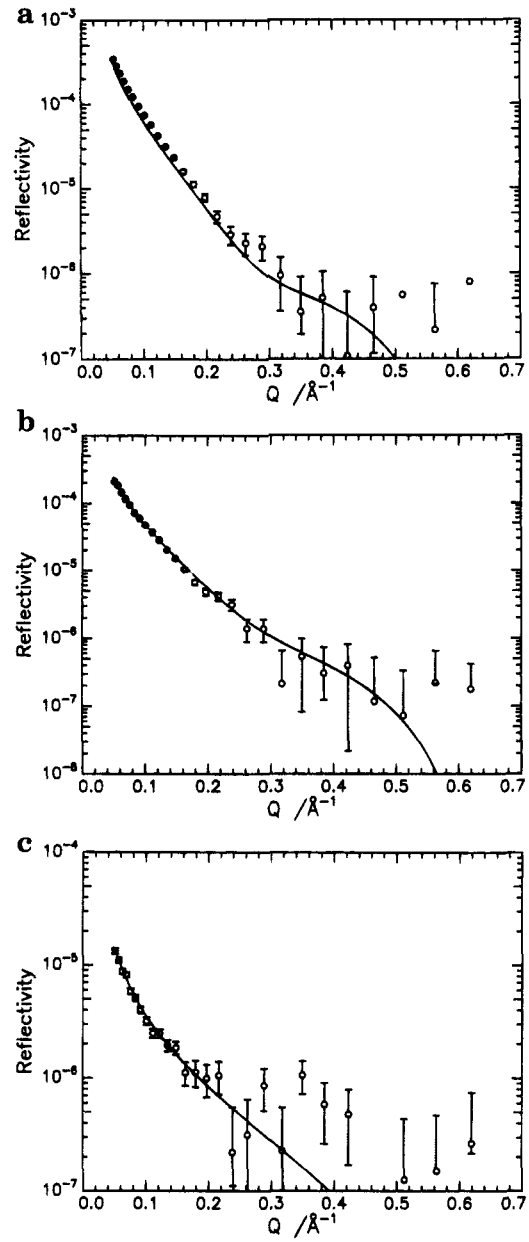

Figure 6. Two-layer fits for PLMA on NRW at a surface pressure of 9 mN m^{-1} from which the optimized parameters given in Table 3 were obtained: (a) DMDL; (b) HMDL; (c) DMHL.

that from the value obtained for the upper layer it must contain a proportion of subphase since the fitted scattering length density is less than that of the pure deuterio lauryl substituent. Furthermore, it is evident from the fitted scattering length density for the lower (backbone) layer that this layer contains an appreciable quantity of subphase because the scattering length density is much reduced from that of the deuterated backbone. Similar logic can be applied to the parameters obtained for the HMDL spread polymer on NRW. We remark here that we have made no allowance for any surface roughness at the air−water interface arising from capillary waves. The properties of these waves have been studied by us using surface quasi-elastic light scattering, and surface viscoelastic parameters have been evaluated.[33] Additionally, we have not included a diffuse change in concentration between the layers in attempting to discern a coarse-grained model of the arrangement of the molecule at the air−water interface. The existence of capillary waves and such diffuse regions do not alter the conclusions made using the

idealized two-layer model, and we have not pursued the inclusion of such aspects in view of our use of the kinematic approximation detailed below.

This process of breaking the near surface layer up into a number of lamellar regions of varying composition and thickness could be continued to provide a complete description of the spread polymer film. However, for more than four such layers the procedure becomes extremely lengthy, and each additional feature must be tested for self-consistency by ensuring that when applied to each combination of polymer and subphase, the results obtained in terms of layer thickness and layer composition are in agreement with each other. This type of analysis has been used to great success by Styrkas et al.[34] in obtaining the organization of polymeric alkylpyridinium monolayers from X-ray reflectivity data.

This iterative method of using the optical matrix calculations is encapsulated in the partial structure factor approach, wherein six equations of the type shown in eq 6 are set up and solved simultaneously at each value of Q to provide the six separate partial structure factors. In addition to providing the thickness of each near surface layer, the partial structure factors also provide the separation between each layer via the cross partial structure factors. This information does not come directly from optical matrix calculations but is deducible with effort. We repeat here that the partial structure factor approach is based on the kinematic *approximation* and thus is confined to reflectivity values of 10^{-2} and below. All of our reflectivity data fulfil this condition and we have solved the simultaneous equations after subtracting the background and correcting the data for polymers spread on D_2O in the manner suggested by Crowley (eq 11).

A model is still required to interpret these partial structure factors. The most commonly applied models are a uniform distribution or a Gaussian distribution of segments at the air–water interface. Due to the limited range of Q accessible (because of background limitations), *either* model would fit the partial structure factor data equally well. However, given the apparent absence of any sharp interfaces and the ability of Gaussian functions to describe polymer probability density functions with acceptable accuracy, we have used the Gaussian distribution model here. For this model

$$n_i(z) = n_{ii} \exp(-4z^2/\sigma^2) \tag{13}$$

where σ is the full width of the distribution where it has fallen to a value of n_{ii}/e, with n_{ii} being the maximum of the number density distribution. The one-dimensional Fourier transform yields the partial structure factor

$$h_{ii}(Q) = n_{ii}\frac{2\pi\sigma^2}{4}\exp\left(\frac{-Q^2\sigma^2}{8}\right) \tag{14}$$

If the Gaussian model is valid, then eq 14 can be rearranged to give

$$\ln h_{ii}(Q) = \ln\left(n_{ii}\frac{2\pi\sigma^2}{4}\right) - \frac{Q^2\sigma^2}{8} \tag{15}$$

A plot of the left-hand side of this equation as a function of Q^2 (a Guinier plot) should be linear with a slope of $-\sigma^2$ and from the intercept a value of n_{ii} can be obtained. Plots of the partial structure factors according to eq 15 are shown in Figure 7 and linear plots are clearly

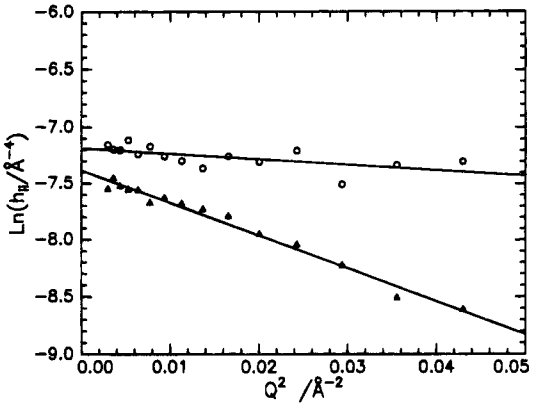

Figure 7. Guinier plots of the self partial structure factors of the backbone (○) and substituent segments (△).

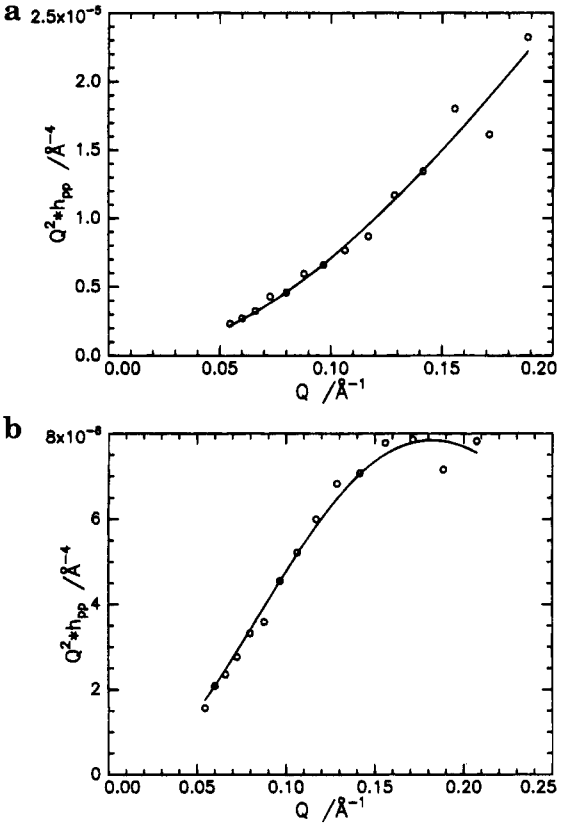

Figure 8. Self partial structure factors for backbone and substituent segments. In each case the solid line is a least squares fit to the data using the Gaussian model discussed. (a) Backbone self partial structure factor; (b) substituent self partial structure factor.

Table 4. Parameters Obtained from Model Interpretation of Partial Structure Factors

π/mN m^{-1}	n_{bi}/ 10^{-3} Å^{-3}	σ_b/ Å	n_{ci}/ 10^{-3} Å	σ_c/ Å	ξ/ Å	δ_{bw}/ Å	δ_{cw}/ Å	δ_{bc}/ Å
5	4	9	1.9	13	3		5	3
9	4.9	6.5	1.8	16	2.5	2	6	3

obtained. Equation 14 can also be nonlinearly least squares fitted (Figure 8) to the self partial structure factors with n_{ii} and σ as the adjustable fitting parameters. Either method gives essentially identical values of n_{ii} and σ within experimental error, and these are given in Table 4.

The cross partial structure factor between the methacrylate backbone and lauryl substituent contains information about the separation between the centers of the two distributions. This cross partial structure factor is given by

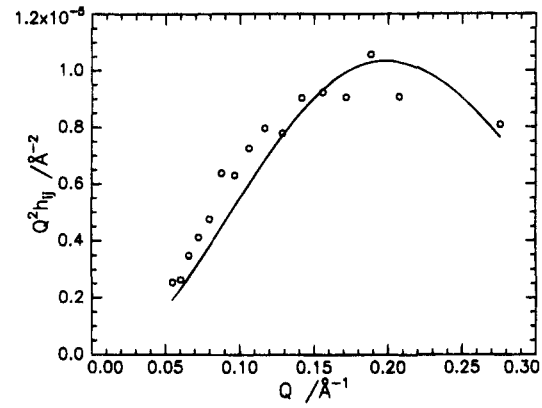

Figure 9. Cross partial structure factor between backbone and substituent segments. The solid line is the best fit using 16 and adjusting the separation between the two distributions.

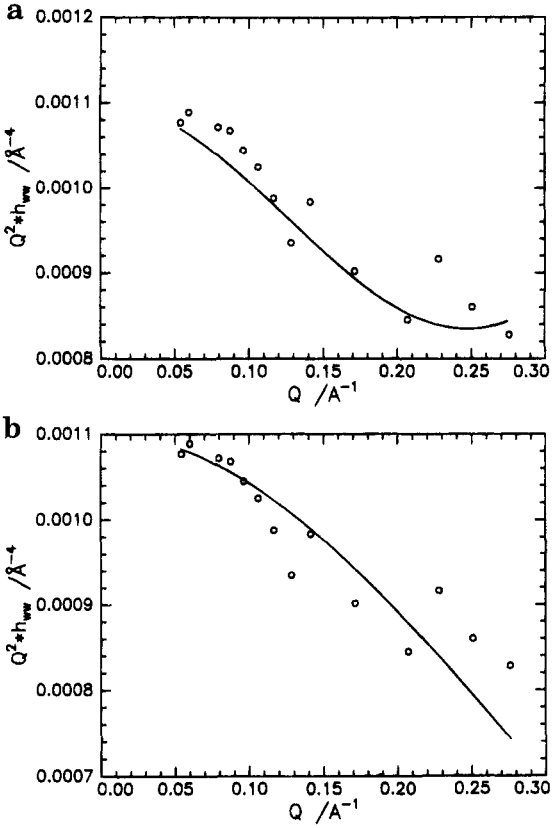

Figure 10. Self partial structure factors for the near surface water layer: (a) fit of a uniform layer to the date; (b) fit of a tanh distribution to the data.

$$h_{bc}(Q) = \pm(h_{bb}(Q)h_{cc}(Q))^{1/2}\cos(Q\delta_{bc}) \qquad (16)$$

where δ_{bc} is the center-to-center separation of the distributions of the backbone and lauryl substituent distributions. The $\pm$ in eq 16 is included to indicate the uncertainty about the phase of the right-hand side, i.e., which layer is uppermost. To obtain δ_{bc} we have used values of $h_{bb}(Q)$ and $h_{cc}(Q)$ calculated using the theoretical Gaussian expression (eq 14) and the parameters given in Table 4. Values of δ_{bc} were adjusted to give the best fit to the values of $h_{bc}(Q)$ obtained from the reflectivity data. Figure 9 shows the least squares fit of the calculated cross partial structure factor to the experimental data. The shape of the cross partial structure factor is obtained but the fitted cross partial structure factor crosses the data. Table 4 includes the value of δ_{bc} from this least squares fit, but changing the value of δ_{bc} by ± 1 Å does not improve the fit to the experimental cross partial structure factor. Furthermore, using experimental values of $h_{bb}(Q)$ and $h_{cc}(Q)$ in place of calculated partial structure factors produces no improvement.

The self partial structure factor for the near surface water layer is shown in Figure 10. Two models are available for the number density distribution of water: a uniform layer with a thickness d and number density n_{wi} over the region $-d/2$ to $d/2$. The partial structure factor for this model is given by

$$h_{ww}(Q) = \frac{1}{Q^2}\left[{n_{wo}}^2 + 4n_{wi}(n_{wi} - n_{wi})\sin^2\left(\frac{Qd}{2}\right)\right] \qquad (17)$$

with n_{wo} the bulk number density of D_2O (3.31×10^{-2} Å^{-3}). For the situation where a more gradual decay of number density prevails, a tanh density profile may be more appropriate:

$$n_{wi}(z) = n_{wo}\left[0.5 + 0.5\tanh\left(\frac{z}{\xi}\right)\right] \qquad (18)$$

where ξ is the characteristic width of the distribution. Neither function produces an excellent fit to the data but the hyperbolic tangent profile is marginally better statistically; moreover, it is physically more realistic. The value of ξ obtained for a surface pressure of 9 mN m^{-1} is 2.5 Å. Using these data in conjunction with the parameters of the Gaussian distributions of the backbone and lauryl substituents, we have obtained the separation between the backbone and subphase as well as the substituent and subphase using the relation

$$h_{iw}(Q) = \pm[h_{ii}(Q)h_{ww}(Q)]^{1/2}\sin(Q\delta_{iw}) \qquad (19)$$

Values of δ_{iw} were varied until the best fit of the right-hand side of eq 19 with the experimental of $h_{iw}(Q)$ were obtained. Figure 11 shows the fits obtained, and the values of δ_{iw} are reported in Table 4. Table 4 also reports values of the various parameters obtained at a surface pressure of 5 mN m^{-1}.

We point out here that n_{bi} and σ_b values for a surface pressure of 5 mN m^{-1} are rather tentative since the reflectivity for the DMHL polymer on NRW is very low and consequently the partial structure factor data for the backbone are rather scattered. Figure 12 shows the backbone segment and lauryl substituent distributions at the water surface. The midpoint of the tanh distribution of water has been arbitrarily placed at $z = 0$. From the cross partial structure factor between the backbone and subphase, a center-to-center separation of ~2 Å is indicated. Combining this with the knowledge that the scattering length density value for the backbone layer from the optical matrix fits suggests a large amount of water is in the layer and the separation from the center of the lauryl substituent distribution (~3 Å), then placements shown in Figure 12a are arrived at. A notable feature of this structural arrangement is that the backbone segments are almost completely immersed in the aqueous subphase and part of the lauryl substituent is also in the aqueous subphase. This backbone immersion is completely different for the organization observed in spread poly(methyl methacrylate) layers. To some extent, this increased immersion of the backbone will be due to the minimization of contact between the hydrophobic lauryl substituent and the aqueous subphase. However, we point out that the description given here is much more detailed than that of our earlier report on poly(methyl methacrylate). This earlier work was unable to use the full power of the

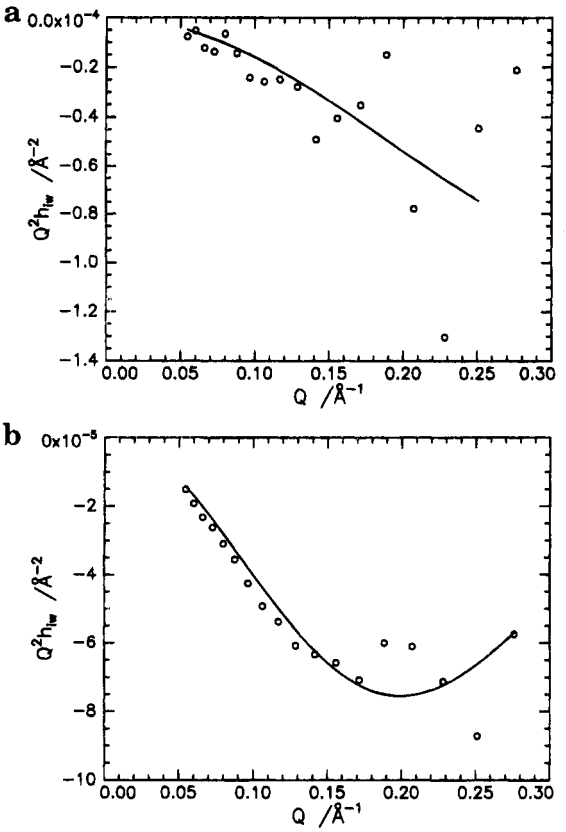

Figure 11. Cross partial structure factors between backbone segment and water (a) and between substituent segments and water (b). In each case the solid line is the best least squares fit calculated using eq 19.

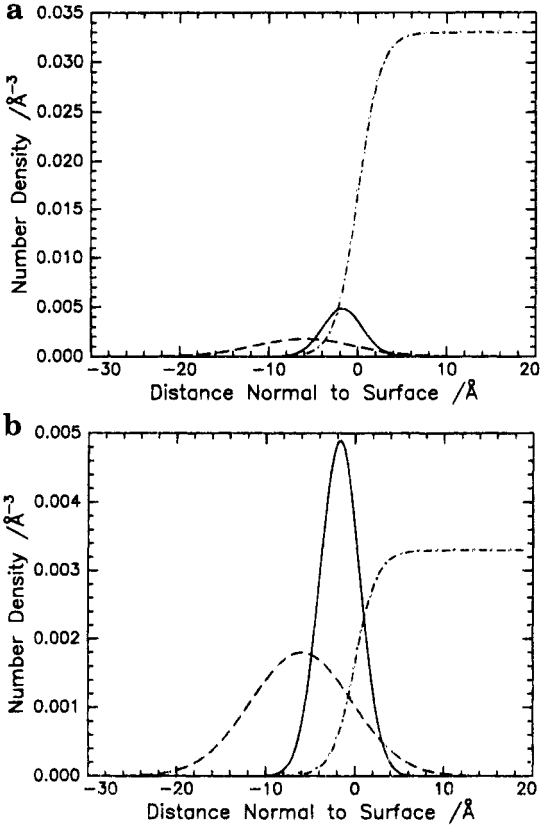

Figure 12. Segment density distributions predicted by the parameters obtained from the partial structure factor analysis of the reflectivity data at 9 mN m^{-1}: (a) as obtained; (b) with water number density divided by 10. Key: (—) methacrylate backbone; (– – –) lauryl substituent; (—·—) water.

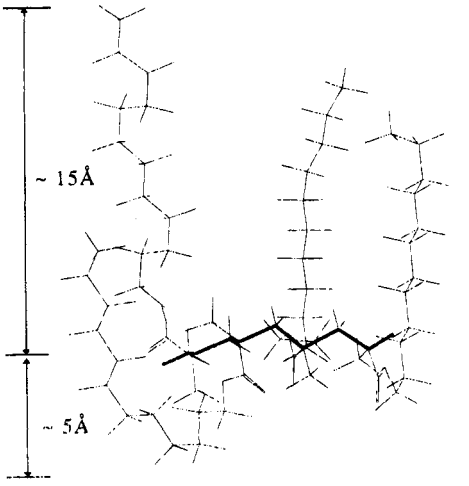

Figure 13. Atomistic stick model of the arrangement of PLMA at the air/water interface based on minimization of configurational energy of a short sequence of the polymer chain. Heavy lines indicate main chain backbone bonds.

kinematic approximation due to the lack of partially deuterated isomers of poly(methyl methacrylate). Furthermore, because of the low level of deuteration in the methyl side chain in such a partially deuterated poly(methyl methacrylate), the reflectivity would be rather small and this would invoke considerable error in the kinematic approximation analysis. The lauryl substituents appear to extend deeper into the subphase than the more polar backbone. Figure 12b shows these distributions in greater detail; the penetration of finite amounts of lauryl substituents to depths of ca. 8–10 Å is clearly evident. A priori this penetration depth for the lauryl side chains is surprising. It can, however, be rationalized (albeit qualitatively) with the equilibrium stereochemical configuration of PLMA. Minimization of the configurational potential energy of four monomer units in a chain sequence of PLMA results in a rotational angle of ±120° (all-trans configuration has a rotational angle of 0°). This forces the lauryl segments to a lower spatial plane than the main chain segments and hence the lauryl segments sample slightly greater depths than the main chain backbone before sufficient rotations about the bonds in the lauryl substituent enable the hydrophobic methylene units to leave the subphase and protrude into the air. With the main chain backbone being almost completely immersed in the subphase, such a configuration means that there will be a region where both lauryl substituents and the main chain backbone are in the same plane and hence there is some penetration of the lauryl units by the subphase. Figure 13 is an attempt to sketch an atomistic arrangement of such a short chain section based on the minimization of the configurational energy; it is evident that a finite amount of the lauryl side chains are in the same plane and slightly below the plane of the main chain backbone. The thicknesses of the two regions which would correspond to the lauryl substituent distribution and the backbone distribution regions are indicated on the figure; although not in exact agreement with experimental values, they are of the same magnitude, and since the calculation on which Figure 13 is based takes no account of polymer–water interactions, this seems a reasonable schematic sketch of the arrangement of PLMA at the air–water interface. For the two surface pressures of the spread PLMA film investigated by us, the change in the value of σ (which is related to the layer thickness) of the lauryl substituent layer is not very great (13 compared to 16 Å) but it is outside the error associated with kinematic approximation analysis of ±1 Å. The "straightening" of

the lauryl side chains with increased surface concentration appears to be small.

The integrated area of the distribution curves for backbone segments and lauryl substituents should be equal if the distributions are an accurate representation of the near surface organization of the polymer. For the distribution curves obtained at a surface pressure of 9 mN m^{-1} separate integrations give a value of 0.026 ± 0.001 backbone segments or lauryl substituents $Å^{-2}$. Consequently, the area per monomer unit calculated from this figure is 38.5 ± 1.5 $Å^2$. From the surface pressure isotherm (Figure 1), the surface concentration at a surface pressure of 9 mN m^{-1} is ca. 1.3 mg m^{-2}, which corresponds to an area per monomer unit of 32 $Å^2$, which is in satisfying agreement with that obtained from the neutron reflectometry data. Note there is a significant uncertainty in the area per monomer unit calculated from the surface pressure isotherm because of the "flat" dependence of surface pressure on surface concentration in this region. The area per monomer unit calculated from the segment distributions will be more accurate. For a surface pressure of 5 mN m^{-1}, integration of the lauryl substituent distribution gives 0.022 $Å^{-2}$, whereas the same type of integration for the backbone segments produces a value of 0.032 $Å^{-2}$. The former value corresponds to a surface area per monomer unit of 45.4 $Å^{-2}$, the latter value to 31.25 $Å^{-2}$. Surface pressure isotherm data suggest the area per monomer unit is approximately 45 $Å^{-2}$ at this surface pressure. This disparity in values obtained from the two distributions has been mentioned earlier. It is solely due to the very weak reflectivity of the DMHL polymer on NRW which results in considerable uncertainty when fitting the partial structure factor. The factor most influenced is the value of σ_b, and since the surface concentration does not change significantly between surface pressures of 5 and 9 mN m^{-1}, we suspect that the true value of σ_b is nearer 6 Å than 9 Å.

Conclusions

Applying neutron reflectometry to a series of partially deuterium-labeled poly(lauryl methacrylates) spread at the air–water interface has resulted in a complete specification of the organization of the molecule at a surface pressure of 9 mN m^{-1}. The methacrylate backbone is essentially wholly immersed in the aqueous subphase, forming a narrow region which can be described by a Gaussian distribution of segments with a standard deviation of ca. 6 Å. The lauryl substituents have the greater part out in the air phase but a considerable amount is immersed in the aqueous subphase and extends some little way deeper into the subphase. This can be attributed to the equilibrium configuration of the segments of the polymer. To relieve steric hindrance, rotations about main chain bonds critically force some of the lauryl substituent deeper into the subphase. Rotations about bonds in the lauryl subgroup eventually enable the hydrophobic substituent to reach the air phase. Cross partial structure factors have been used to determine the separation between the main chain and the substituent and between each component of the polymer and the subphase. Integration of the separation distributions produces identical number of segments per unit area, a number which agrees well with that derived from the surface pressure isotherm.

This description is little altered for the lower surface pressure of 5 mN m^{-1} except that the backbone segment distribution is slightly less certain due to the very low reflectivity of one of the partially labeled polymers.

Acknowledgment. I.R. thanks EPSRC for the provision of a maintenance grant. R.W.R. and I.R. thank EPSRC for having the foresight to construct the ISIS pulsed neutron facility.

References and Notes

(1) des Cloizeaux, J.; Jannink, G. *Polymers in Solution: Their Modelling and Structure*; Oxford University Press: Oxford, 1987.
(2) Cohen-Stuart, M. A.; Fleer, G. J.; Scheutjens, J. H. M.; Cosgrove, T.; Vincent, B. *Polymers at Interfaces*, 1st ed.; Chapman & Hall: London, 1993.
(3) Hodge, P.; Ali-Adib, Z.; West, D.; King, T. *Macromolecules* **1993**, *26*, 1789.
(4) Motomura, K.; Matuura, R. *J. Colloid Sci.* **1963**, *18*, 52.
(5) Shuler, R. L.; Zisman, W. A. *J. Phys. Chem.* **1970**, *74*, 1523.
(6) Peng, J. B.; Barnes, G. T. *Langmuir* **1991**, *7*, 1749.
(7) Peng, J. B.; Barnes, G. T. *Langmuir* **1990**, *6*, 578.
(8) Peng, J. B.; Barnes, G. T. *Langmuir* **1991**, *7*, 3090.
(9) Vilanove, R.; Rondelez, F. *Phys. Rev. Lett.* **1980**, *45*, 1502.
(10) Vilanove, R.; Poupinet, D.; Rondelez, F. *Macromolecules* **1988**, *21*, 2491.
(11) Poupinet, D.; Vilanove, R.; Rondelez, F. *Macromolecules* **1989**, *22*, 2491.
(12) Kawaguchi, M.; Yoshida, A.; Takahashi, A. *Macromolecules* **1983**, *16*, 956.
(13) Takahashi, A.; Yoshida, A.; Kawaguchi, M. *Macromolecules* **1982**, *15*, 1196.
(14) Brinkhuis, R. H. G.; Schoutjens, A. H. G. *Macromolecules* **1992**, *25*, 2732.
(15) Brinkhuis, R. H. G.; Schoutjens, A. H. G. *Macromolecules* **1992**, *25*, 2717.
(16) Sauer, B. B.; Yu, H.; Yazdanian, M.; Zografi, G.; Kim, M. W. *Macromolecules* **1989**, *22*, 2232.
(17) Kawaguchi, M.; Saito, W.; Kato, T. *Macromolecules* **1994**, *27*, 5882.
(18) Motschmann, H.; Reiter, R.; Laurall, R.; Duda, G.; Stamm, M.; Wegner, G.; Knoll, W. *Langmuir* **1991**, *7*, 2743.
(19) Simister, E. A.; Lee, E. M.; Thomas, R. K.; Penfold, J. *J. Phys. Chem.* **1992**, *96*, 1373.
(20) Lu, J. R.; Li, Z. X.; Su, T. J.; Thomas, R. K.; Penfold, J. *Langmuir* **1993**, *9*, 2408.
(21) Thomas, R. K. In *Scattering Methods in Polymer Science*; Richards, R. W., Ed.; Prentice-Hall: Englewood Cliffs, NJ, 1995; Chapter 4.
(22) Henderson, J. A.; Richards, R. W.; Penfold, J.; Thomas, R. K. *Macromolecules* **1993**, *26*, 65.
(23) Henderson, J. A.; Richards, R. W.; Penfold, J.; Thomas, R. K.; Lu, J. R. *Macromolecules* **1993**, *26*, 4591.
(24) Henderson, J. A.; Richards, R. W.; Penfold, J.; Thomas, R. K. *Acta Polym.* **1993**, *44*, 184.
(25) Richards, R. W.; Rochford, B. R.; Webster, J. R. P. *Discuss. Faraday Soc.* **1995**, *98*.
(26) Lu, J. R.; Simister, E. A.; Lee, E. M.; Thomas, R. K.; Rennie, A. R.; Penfold, J. *Langmuir* **1992**, *8*, 1837.
(27) Lu, J. R.; Lee, E. M.; Thomas, R. K.; Penfold, J.; Flitsch, S. L. *Langmuir* **1993**, *9*, 1352.
(28) Lekner, J. *Theory of Reflection*; Nijhof: Dordrecht, 1987.
(29) Crowley, T. L. *Physica A* **1993**, *95*, 354.
(30) Penfold, J.; Thomas, R. K. *J. Phys. Condens. Matter* **1990**, *2*, 1369.
(31) Granick, S.; Clarson, S. J.; Formoy, T. R.; Semlyen, J. A. *Polymer* **1985**, *26*, 925.
(32) Henderson, J. A.; Richards, R. W.; Penfold, J.; Shackleton, C.; Thomas, R. K. *Polymer* **1991**, *32*, 3284.
(33) Reynolds, I., unpublished results.
(34) Styrkas, D. A.; Thomas, R. R.; Adib, Z. A.; Davis, F.; Hodge, P.; Liu, X. H. *Macromolecules* **1994**, *27*, 5504.

MA950582I